ACCOUNTS of chemical research

Article

pubs.acs.org/accounts

Contorted Polycyclic Aromatics

Melissa Ball,[‡] Yu Zhong,[‡] Ying Wu,[‡] Christine Schenck,[‡] Fay Ng,*[,‡] Michael Steigerwald,*[,‡] Shengxiong Xiao,*[,†] and Colin Nuckolls*[,‡,†]

[†]The Education Ministry Key Lab of Resource Chemistry, Shanghai Key Laboratory of Rare Earth Functional Materials, Optoelectronic Nano Materials and Devices Institute, Department of Chemistry, Shanghai Normal University, Shanghai 200234, China

[‡]Department of Chemistry, Columbia University, New York, New York 10027, United States

CONSPECTUS: This Account describes a body of research in the design, synthesis, and assembly of molecular materials made from strained polycyclic aromatic molecules. The strain in the molecular subunits severely distorts the aromatic molecules away from planarity. We coined the term "contorted aromatics" to describe this class of molecules. Using these molecules, we demonstrate that the curved pi-surfaces are useful as subunits to make self-assembled electronic materials. We have created and continue to study two broad classes of these "contorted aromatics": discs and ribbons. The figure that accompanies this conspectus displays the three-dimensional surfaces of a selection of these "contorted aromatics".

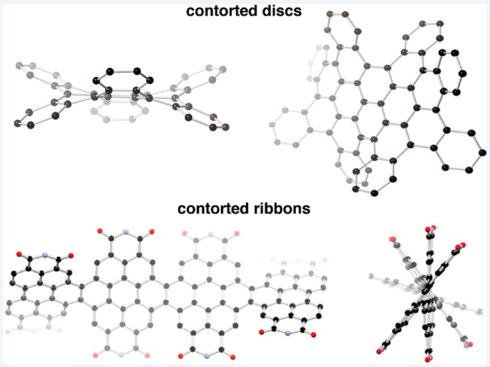

The disc-shaped contorted molecules have well-defined conformations that create concave pi-surfaces. When these disc-shaped molecules are substituted with hydrocarbon side chains, they self-assemble into columnar superstructures. Depending on the hydrocarbon substitution, they form either liquid crystalline films or macroscopic cables. In both cases, the columnar structures are photoconductive and form p-type, hole-transporting materials in field effect transistor devices. This columnar motif is robust, allowing us to form monolayers of these columns attached to the surface of dielectrics such as silicon oxide. We use ultrathin point contacts made from individual single-walled carbon nanotubes that are separated by a few nanometers to probe the electronic properties of short stacks of a few contorted discs. We find that these materials have high mobility and can sense electron-deficient aromatic molecules.

The concave surfaces of these disc-shaped contorted molecules form ideal receptors for the molecular recognition and assembly with spherical molecules such as fullerenes. These interfaces resemble ball-and-socket joints, where the fullerene nests itself in the concave surface of the contorted disc. The tightness of the binding between the two partners can be increased by creating more hemispherically shaped contorted molecules. Given the electronic structure of these contorted discs and the fullerenes, this junction is a molecular version of a p−n junction. These ball-and-socket interfaces are ideal for photoinduced charge separation. Photovoltaic devices containing these molecular recognition elements demonstrate approximately two orders of magnitude increase in charge separation.

The ribbon-shaped, contorted molecules can be conceptualized as ultranarrow pieces of graphene. The contortion causes them to wind into helical ribbons. These ribbons can be formed into the active layer of field effect transistors. We substitute the ribbons with di-imides and therefore are able to transport electrons. Furthermore, these materials absorb light strongly and have ideal energetic alignment of their orbitals with conventional p-type electronic polymers. In solar cells, these contorted ribbons with commercial donor polymers have record efficiencies for non-fullerene-based solar cells. An area of interest for future exploration is the merger of these highly efficient contorted ribbons with the well-defined interfaces of the ball-and-socket materials.

INTRODUCTION

Here, we describe a body of research in the design, synthesis, and study of strained polycyclic aromatics. We named these compounds "contorted aromatics" because steric congestion in their periphery results in nonplanar structures. The contorted structure has important ramifications on the inherent physical behavior of these materials. The intermolecular contacts in crystals and polycrystalline films are versatile relative to those available to flat aromatics, and, consequently, their charge transport properties in organic materials-based devices can be improved. In addition, the nonplanar structures provide concave surfaces that recognize the convex surfaces of fullerenes. This mode of self-assembly makes them useful in creating atomically defined p−n junctions in organic photovoltaics. Finally, these materials are more soluble and less likely to spontaneously aggregate compared to flat aromatics, allowing for solution-based processing of materials.

It is important to put this body of research into context within organic materials research. The molecules described here are elements of nanostructured carbon-based materials. They are model systems and potential seeds for the synthesis of

Received: September 30, 2014
Published: December 19, 2014

   dx.doi.org/10.1021/ar500355d | *Acc. Chem. Res.* 2015, 48, 267−276

nanotubes, graphene, and fullerenes.[1−5] These molecules and the understanding of their properties inform and provide a counterpoint to studies on flat aromatics.[2] Moreover, the molecules described here are influenced by plastic electronic materials, but, in this case, molecular recognition events and self-assembly processes transform them from molecules to materials.[6]

The molecular feature incorporated into the design of these contorted structures is benzophenanthrene (Figure 1A), also

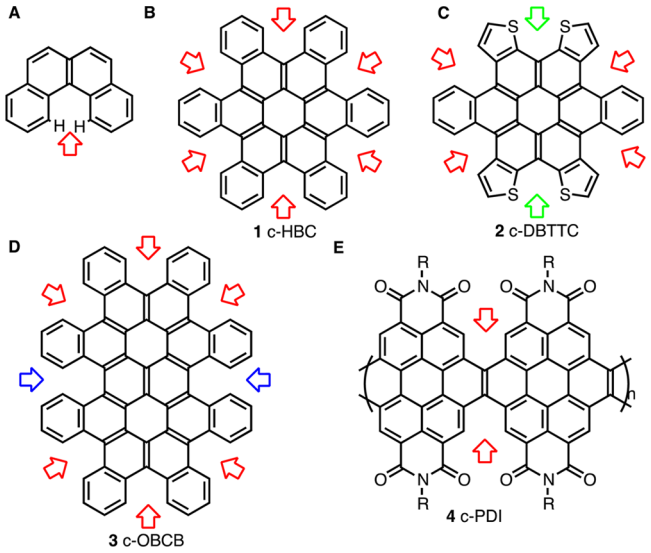

Figure 1. (A) Benzophenanthrene. (B) c-HBC, **1**. Red arrows show the cove regions benzophenanthrene subunits. (C) c-DBTTC, **2**. Green arrows for similar interactions with thiophene rings. (D) c-OBCB, **3**. Blue arrows indicate the fjord regions of the [5]-helicenes. (E) c-PDI, **4**.

known as [4]-helicene.[7] A highly nonplanar molecule results from the steric congestion in the cove positions. Benzophenanthrene has a splay angle of 19.9° and a barrier for inversion between the two helices of 7.6 kcal/mol.[8] The contorted hexabenzocoronene (**1** c-HBC, Figure 1B) is conceptually the superposition of six benzophenanthrene subunits into a hexagonal array.[9] Substituting four benzo groups with thiophenes creates the heteroaromatic contorted dibenzotetrathienocoronene (**2** c-DBTTC, Figure 1C).[10] Extending the core along one axis generates the contorted octabenzocircumbiphenyl (**3** c-OBCB, Figure 1D).[11] Continuing with this motif, we created one-dimensional systems that incorporate these subunits into ribbons that are synthesized from perylene-3,4,9,10-tetracarboxylic acid diimide (**4** c-PDI, Figure 1E).[12] This Account describes the structure, assembly, and properties of this new class of molecules.

STRUCTURE

Contorted Hexabenzocoronene

The harsh conditions of the first synthesis of c-HBC (**1**) precluded an in-depth study of these molecules.[13] We developed an approach that allows a wealth of derivatives to be readily synthesized and investigated.[9] Recently, others[14−18] have created complementary methods that incorporate further diversity within the c-HBCs. Figure 2 shows the structure of **1** deduced from single-crystal X-ray diffraction. The structure adopts a conformation where the exterior benzo-groups fold

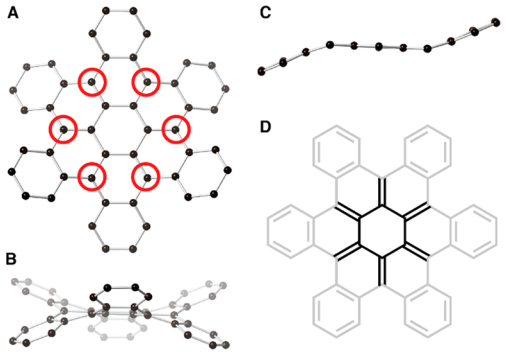

Figure 2. Crystal structure of c-HBC **1** with hydrogens removed. (A) Face-on view with the pivot points marked (red circles). (B) Side-on view. (C) Side-on view of one of the acene segments extracted from the crystal structure. The other atoms are hidden. (D) Radialene resonance form. Adapted with permission from ref 9. Copyright 2005 WILEY-VCH Verlag GmbH & Co. KGaA.

alternately above or below the pi-plane, creating two concave surfaces (Figure 2).[9] The majority of the bending is concentrated in carbons (circled in red) that act as pivot points (Figure 2A).

In addition to the unique structure adopted by the c-HBC molecules, the crystal structure also demonstrates a strong contribution from the radialene resonance structure (Figure 2D).[20] Spectroscopic measurements and density functional theory (DFT) support the existence of two pi-systems attributed to a relatively lower energy radialene core and higher energy out-of-plane phenyl rings.[19]

Calculations support that the up−down conformation is the lowest energy conformer by a substantial margin for c-HBC's core. We observe this conformation for many substituted derivatives of c-HBC. As a result, we were surprised when we obtained the crystal structure of a derivative of the c-HBC substituted with 16 fluorines, whose central acene subunit adopts a bowed structure (Figure 3). Experimentally, this structure is higher in energy than that of the up−down conformation.[21]

Heteroaromatic Versions

c-DBTTC (**2**) replaces the peripheral fused benzene rings of c-HBC with thiophene rings.[10,22,23] The structure can be viewed as the superposition of two anthradithiophene units and one pentacene unit with the coronene core preserved. The molecular structure of c-DBTTC is flatter than c-HBC due to relaxed steric interactions in the periphery. Calculations (using B3LYP/6-31G) show three distinct conformations. The first two of these predicted conformations are isoenergetic with the circumferential rings, adopting an up−down−up−down−up−down conformation (Figure 4A) and an up−down−down−up−down−down conformation (Figure 4B, butterfly conformation). The third molecular conformation [Figure 4C, the up−down−down−twist−up−down (U−D−D−T−U−D) arrangement] is predicted to be ∼4 kcal/mol higher in energy and has not been observed experimentally.[10]

We observe the up−down and butterfly conformations in crystal structures of derivatives of the c-DBTTCs. When the c-DBTTC molecule is substituted with alkyl chains, its crystal structure simultaneously exhibits both the up−down and butterfly conformations. The crystal structure from the parent, unsubstituted c-DBTTC (**2**), contained only the molecules in an up−down conformation. The packing of **2** is unusual

dx.doi.org/10.1021/ar500355d | Acc. Chem. Res. 2015, 48, 267−276

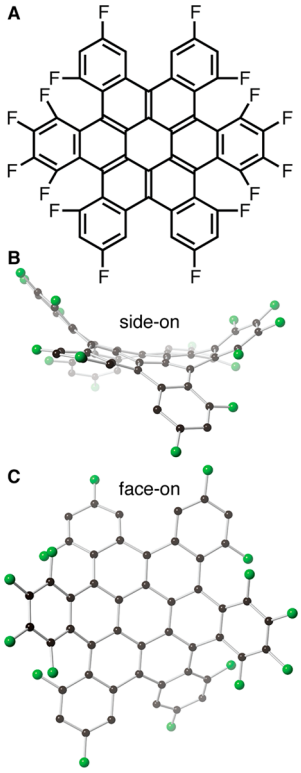

Figure 3. (A) c-HBC with 16 fluorine atoms. (B) Side-on and (C) face-on views from single-crystal X-ray diffraction. Fluorine, green; hydrogens have been removed. Adapted with permission from ref 21. Copyright 2010 American Chemical Society.

because it forms a columnar superstructure where neighboring atoms in the stack almost completely eclipse each other.[10] Typically, when electron-rich aromatics stack cofacially, the atoms are offset from each another.[24,25] The important finding here is that the thiophene units yield a more flexible structure relative to the parent c-HBC and that these contorted heterocyclic aromatics accommodate a wide range of electron acceptors within devices (vide infra).[10,22,26,27]

Expanded Aromatic Cores

c-HBC and c-DBTTC have similar optical and electronic properties. To obtain meaningful electronic changes, we expanded the core to form the c-OBCB (**3**). The absorption spectrum of **3** is red-shifted due to its more accessible frontier orbitals. The c-OBCB (**3**) conformation (Figure 5) is similar to

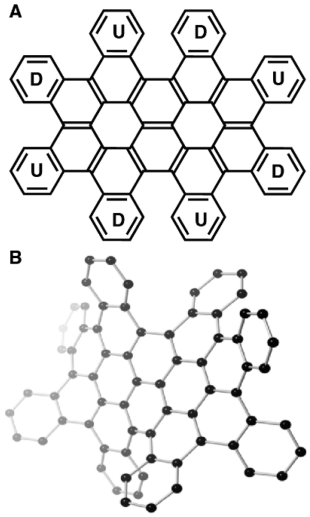

Figure 5. (A) c-OBCB **3** with alternating up (U) and down (D) benzo-rings. (B) DFT-generated structure for **3**. Hydrogens have been removed. Adapted with permission from ref 11. Copyright 2013 Royal Society of Chemistry.

that of the c-HBC, as both contain six benzophenanthrenes arrayed around the exterior of the circumbiphenyl core.[11] Additionally, the c-OBCB has two [5]-helicenes around its exterior, forming a chiral structure.

Molecular Wires of Contorted Aromatics

We have recently created versions of these contorted molecules whose cores can be extended in one direction to make one-dimensional contorted ribbons. We used fused PDIs together to make atomically defined graphene ribbons, the c-PDI family (**4**). Our approach allows for exquisite structural control and versatility to synthesize oligomeric derivatives.[12] There are other related examples of PDI oligomers.[28] Figure 6 shows the three oligomers we synthesized: the dimer ($\mathbf{4}_2$), trimer ($\mathbf{4}_3$), and tetramer ($\mathbf{4}_4$).

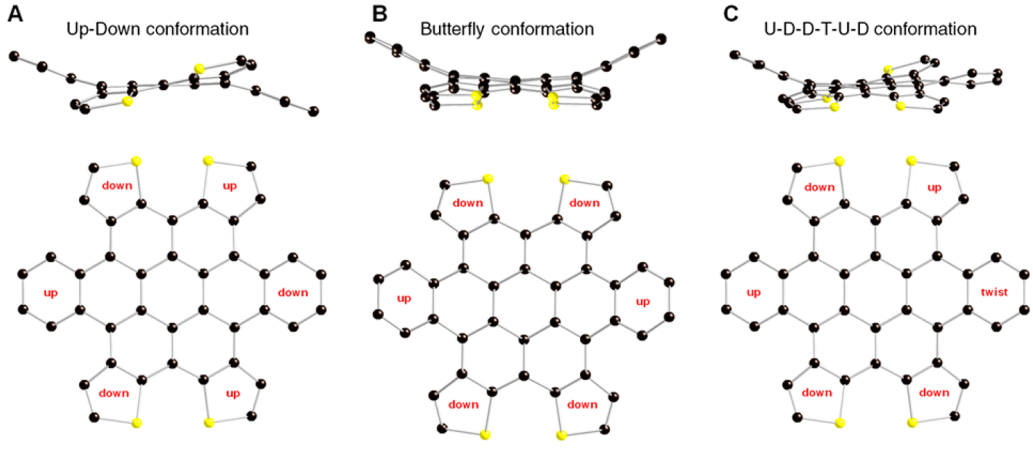

Figure 4. Side and top views of DFT-optimized conformations for **2**. (A) Up−down conformation. (B) Butterfly conformation. (C) UDDTUD conformation. Hydrogen atoms have been removed. Black, carbon; yellow, sulfur. Adapted with permission from ref 10. Copyright 2011 Royal Society of Chemistry.

dx.doi.org/10.1021/ar500355d | Acc. Chem. Res. 2015, 48, 267−276

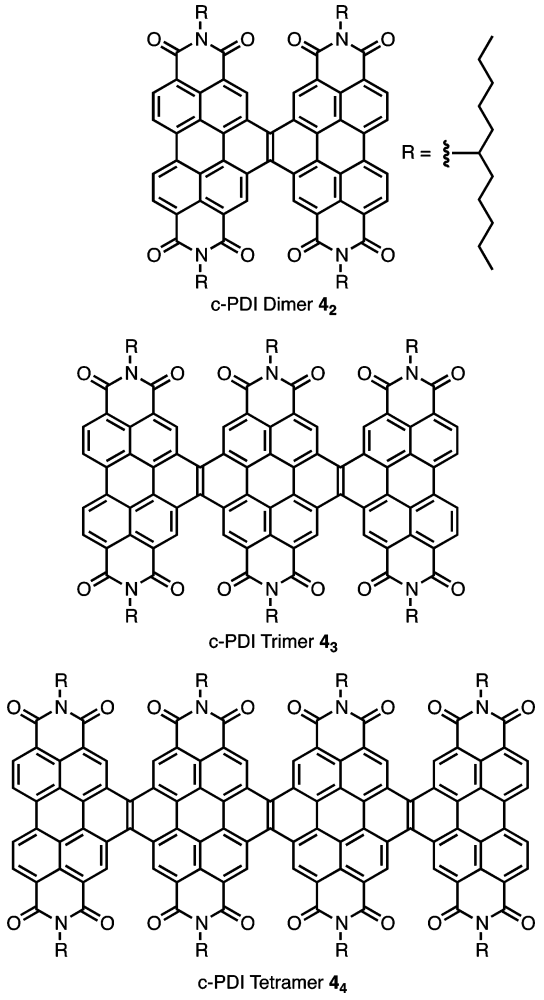

Figure 6. c-PDI, **4**, family of oligomers.

The dimer (4_2) exists in the helical conformation as a pair of enantiomers. As we synthesize longer oligomers, the conformers become more numerous. We identified two conformations possible for the PDI trimer (4_3): helical and waggling (Figure 7A). The tetramer (4_4) also may adopt a helical and waggling conformation, but, now with three ring junctions, there is also a mixed conformation. Calculations (using B3LYP/6-31G) suggest that these conformations are similar in energy. From both ground- and excited-state DFT calculations of **4**, the energy of the HOMO/LUMO excitation decreases with increasing oligomers length, typical for conjugated molecules. Interestingly, we found that the HOMO-2 to LUMO transition also decreased in energy across the oligomer series (Figure 7B).[12] The HOMO-2 orbital is the highest energy occupied orbital associated within the olefin connecting the oligomers, whereas the LUMO is concentrated predominantly within the PDI-subunits. As a result, the HOMO-2 to LUMO transition describes the promotion of an electron from the bridging olefin(s) to the PDI subunits. Within the tetramer, the HOMO/LUMO and HOMO-2/LUMO transitions are approximately isoenergetic, resulting in greatly increased absorption in the visible wavelengths.[12]

SELF-ASSEMBLED MATERIALS

Given the diversity of contorted aromatic molecules we created, we were interested in their ability to transfer charge and function within devices. c-HBC, c-DBTTC, and c-OBCB are electron donors, whereas PDI molecules are electron acceptors. We determined the efficacy of intermolecular charge transport in thin film devices in both organic field effect transistors (OFETs) and organic photovoltaics (OPVs). The nonplanar peripheries and the unique intermolecular contacts available to these contorted molecules allowed us to show that a nonplanar core structure could be efficient at intermolecular charge transport.[29,30]

Columnar Structures and OFETs

Adding alkoxyl chains to the c-HBC creates structures that self-assemble. With 4-dodecycloxy chains (Figure 8A), c-HBC (**1B**) forms a hexagonally ordered columnar liquid-crystalline phase (Figure 8B).[9] The coaxial aromatic core of the stack can act as a conduit for charge, and the exterior of the molecule can behave as an insulating sheath. In cast films, the columns align themselves parallel to the surface, with the discs oriented edge-on to the substrate (Figure 8C). Alignment of the columns parallel to the surface allows charge transport to be probed laterally. Figure 9 shows the electrical current at a constant electrical bias between two parallel electrodes as the films are illuminated. The electrical current retraces the UV−vis absorption spectra and highlights the core and cladding of these stacks.[19]

Figure 9B,C display the OFETs constructed on films of **1B**. It is a p-type, hole-transporting semiconductor and has

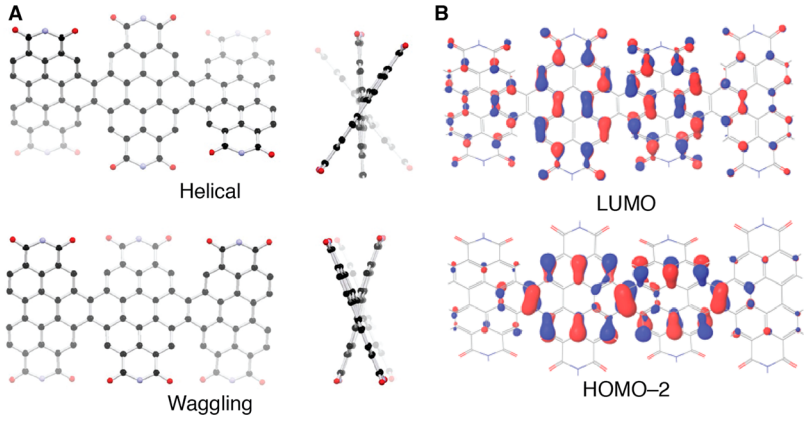

Figure 7. (A) Face-on and side-on views of two conformations from 4_3. (B) HOMO-2 and LUMO of the 4_4. There is no significant change in the energy or the shape of the orbitals for the different conformations. Adapted from ref 12. Copyright 2014 American Chemical Society.

dx.doi.org/10.1021/ar500355d | Acc. Chem. Res. 2015, 48, 267−276

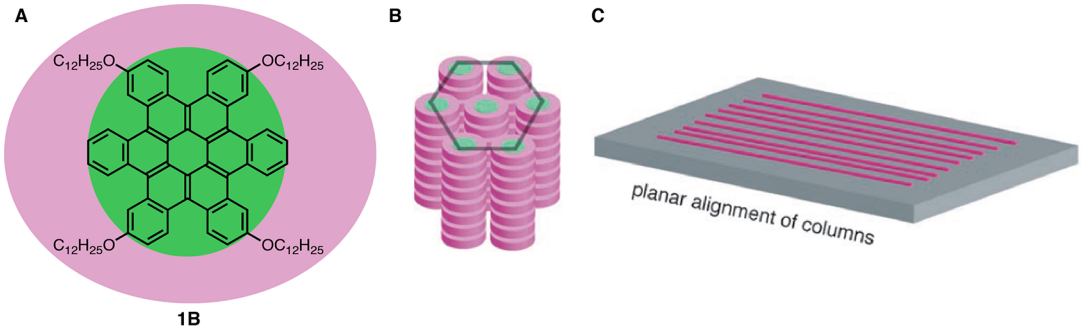

Figure 8. (A) c-HBC **1B**. (B) Columnar, hexagonal arrangement of **1B**. (C) The columns of **1B** align themselves parallel to the substrate. Adapted with permission from ref 9. Copyright 2005 WILEY-VCH Verlag GmbH & Co. KGaA.

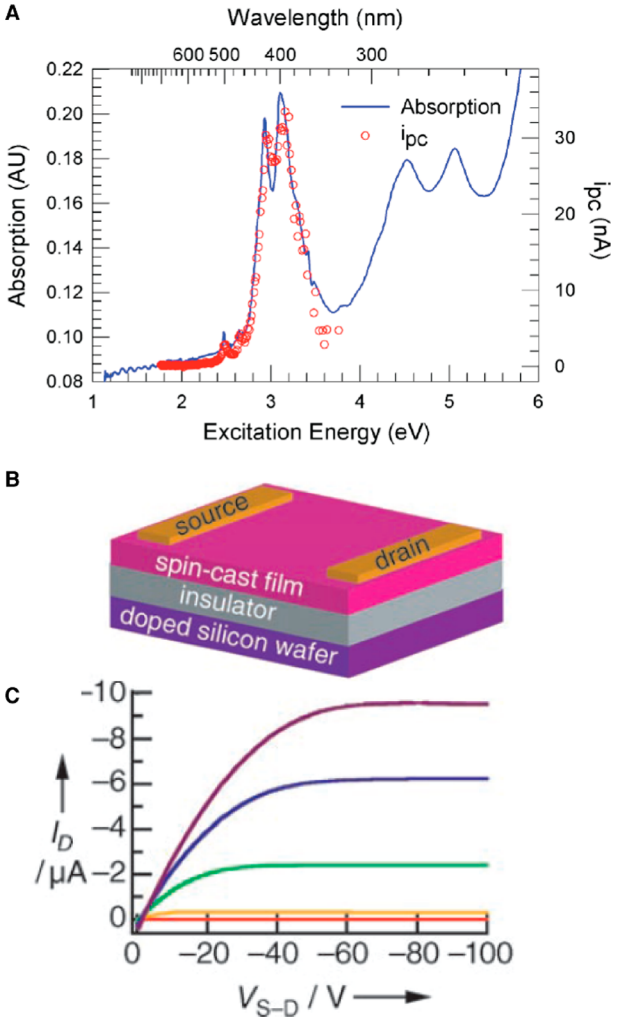

Figure 9. (A) Absorption spectrum (solid line) and photocurrent spectral response (circles) of **1B** in thin-films. (B) OFET fabricated on a film of **1B**. (C) OFET output from **1B**. The gate voltage varied from 20 V (red) to 100 V (purple) in 20 V increments. Adapted with permission from ref 9, Copyright 2005 WILEY-VCH Verlag GmbH & Co. KGaA, and ref 19, Copyright 2006 American Chemical Society.

noteworthy FET characteristics relative to those of other similar materials.[9] Many of the derivatives of the c-HBC, c-DBTTC, and c-OBCB also form p-type materials with similar OFET behavior.[11,31] Interestingly, c-OBCB can be simultaneously switched by using two different inputs: electrical bias and protonation.[32] For example, placing the device (from **3**) in acid vapor can turn on the transistor. The exciting result encompassing this class of materials is that the transistor characteristics are in many cases better than those of the corresponding planar aromatics, reflecting the unique packing of these contorted building blocks.

The mode of self-assembly changes when we substitute c-HBC with 8-dodecyloxy chains (**1C**, Figure 10A). **1C** shows no mesophase but forms orthorhombic crystalline cables.[31] Individual cables can be manipulated with an elastomeric stamp to place them into electrical devices (Figure 10B,C). These individual cables act as p-type semiconducting cables. This procedure is a general method to manipulate and position highly ordered, self-assembled nanostructured materials in devices.

As of yet, c-PDIs' (**4**) packing structure within the films is unknown. The c-PDI molecules make efficacious n-type materials OFETs.[33,34] We also found a modest dependence between the length of the oligomers and the mobility of carriers within the films. Their ability to transfer electrons is interesting given their nonplanar core.

On the basis of the OFET experiments detailed above, our hypothesis was that contorted aromatic molecules' properties were limited by defects, grain boundaries, and other extrinsic factors. To test this assertion, we devised a method to measure properties on an individual stack of molecules composed of only a few molecules. The contacts were made from an individual single-walled carbon nanotube (SWCNT), wired into a device, that had a section excised using lithography.[35,36] The SWCNT point contacts formed the source and drain electrodes and were separated by only a few nanometers (Figure 11A). At most, 20 molecules can span the gap. We made a columnar film of **1B**.[37] This device shows record mobility (>1 $cm^2\ V^{-1}\ s^{-1}$) for an OFET from columnar liquid-crystalline materials.[37]

Monolayers of c-HBC

We also found that we could use these same types of nanotube devices to measure properties on monolayers of the c-HBC that form between the ends of the nanotube. The acid chloride of **1D** reacts with the silicon oxide surface to form a laterally pi-stacked monolayer (Figure 11B).[38] Because it is only a monolayer channel, these FETs were found to be sensitive to other electron-deficient aromatics such as TCNQ and are useful as new types of ultrasensitive environmental and molecular sensors (<0.1 μM analyte sensitivity).[38]

An understanding of how to control assembly at both the dielectric interface and on metal surfaces is important for device optimization. We studied assembly on gold, copper, cobalt, and ruthenium using scanning tunneling microscopy.[39−42] There

dx.doi.org/10.1021/ar500355d | Acc. Chem. Res. 2015, 48, 267−276

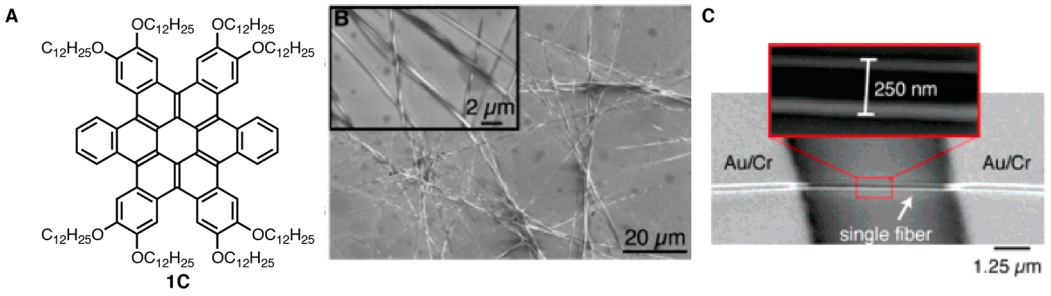

Figure 10. (A) c-HBC **1C**. (B) Scanning electron microscopy image of **1C** organized into nanoscale cables. (C) Individual cables could be put into devices by using an elastomeric stamp. Adapted with permission from ref 31. Copyright 2006 American Chemical Society.

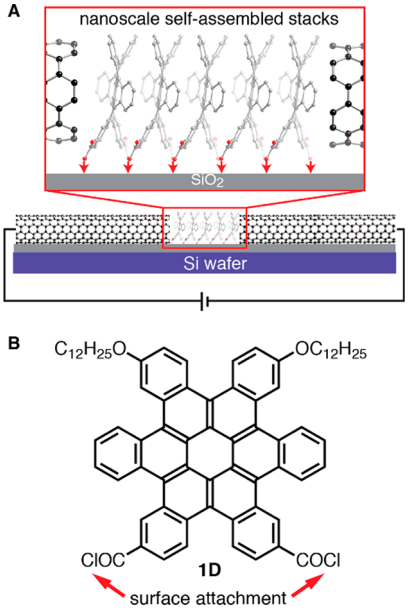

Figure 11. (A) Stack of c-HBCs between SWCNT contacts. (B) **1D** with acid chlorides form a monolayer transistor channel between SWCNT contacts. Adapted with permission from ref 38. Copyright 2006 The National Academy of Sciences of the USA.

was no detectable arrangement of **1** on gold, and on cobalt, **1** was deconstructed and reformed into graphene islands.[39,40] On a crystalline copper surface, **1** forms a honeycomb structure.[41]

When **1** is formed as a submonolayer on ruthenium, we observe the molecule flattening to make contact with the metal, but it is unable to become completely planar and has one arm that remains out the plane of the core (Figure 12).[42] We observe hemispheric HBCs, resulting from the formation of six 5-membered rings, by applying heat to a submonolayer of c-HBCs on ruthenium (Figure 12). This hemispheric form for **1** is significant because of its potential to act as a seed for carbon

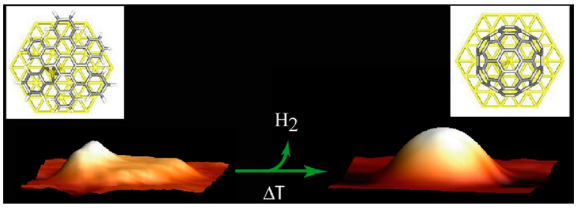

Figure 12. STM image of **1** on a ruthenium surface. Upon heating, a hemispheric molecule forms. Adapted with permission from ref 42. Copyright 2007 WILEY-VCH Verlag GmbH & Co. KGaA.

nanotube growth with a specific chirality and diameter.[43] As the molecules were strongly bound to the metal surface, we developed a solution-based method to investigate their properties further. We synthesized and studied both the two-ring and four-ring closed analogues that also possess a bowl-shaped conformation (Figure 13).[44]

Photovoltaics

Given their unusual shapes and facile charge transport, we were interested in studying these molecules in OPVs. As mentioned above, the contorted disc shaped molecules are good hole-transporting materials.[10,31] c-DBTTC forms a crystalline donor layer of a supramolecularly assembled, three-dimensional network of cables. This scaffold not only facilitates charge transport but also provides a template for a reticulated heterojunction with C_{60}.[26] The nanostructured active layer provides a 3- to 4-fold increase in the power conversion efficiency compared to that of active layers based on the flat analogue.[27]

Self-assembly of the donor and the acceptor on the molecular scale has been proposed to control morphology and improve device performance in the polymer bulkjunctions,[45−48] although molecular examples are rare.[49−51] c-HBC is a perfect partner for fullerenes because they are complementary to each other in size and shape. Co-crystallization occurs both from solution and the vapor phase to form a ball-and-socket arrangement (Figure 14A).[52] We found that a derivative of **2** also co-crystallizes with C_{60} to produce a co-crystal (Figure 14B).[10] This supramolecular arrangement of ball-shaped, n-type semiconductor and bowl-shaped p-type semiconductor arranges them to communicate electronically and imparts the efficacious photovoltaic properties discussed below.

To test whether shape complementarity was important in the devices, we constructed two devices utilizing **1** and a planar HBC.[2] Both molecules share similar electronic and physical properties, with the notable difference being shape. We found that devices made from c-HBC were more efficient relative to the flat HBC by about 2 orders of magnitude greater photon conversion efficiency (PCE).[52] The shape complementary complex yields an intimate donor−acceptor interface that results in enhanced electronic properties.

The ball-and-socket complex also exists in films of both **1B**:$PC_{70}BM$,[53] **2**:$PC_{70}BM$,[22] and **3**:$PC_{70}BM$.[11] Formation of this supramolecular complex affects charge separation in the active layer (Figure 15A), leading to organic solar cells for **1B** in blended film with a maximum PCE of 2.41% (Figure 15B). The PCE is high considering that the absorption of **1B** is largely in the UV range. We observed improved efficiency in a **3**:$PC_{70}BM$ solar cell due to the bathochromic shift of c-OBCB relative to

dx.doi.org/10.1021/ar500355d | Acc. Chem. Res. 2015, 48, 267−276

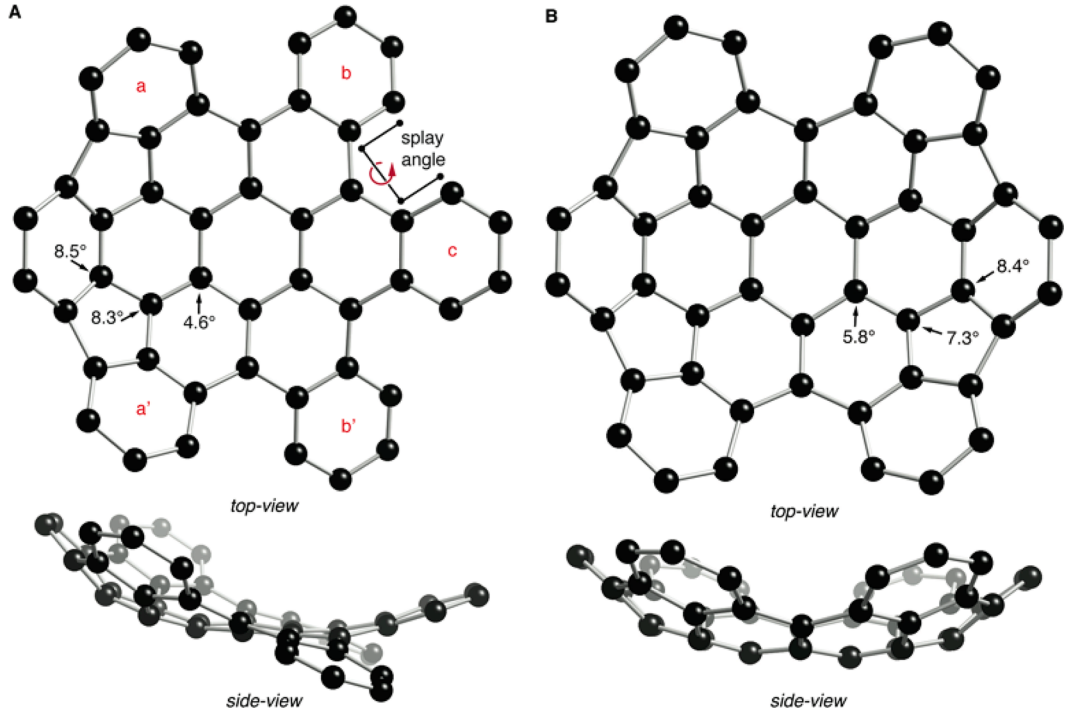

Figure 13. DFT-calculated structure of (A) 2-closed HBC and (B) 4-closed c-HBC. POAV angles at their corresponding carbon atoms. Carbons are shown with black spheres. Hydrogens have been removed. Adapted with permission from ref 44. Copyright 2011 Royal Society of Chemistry.

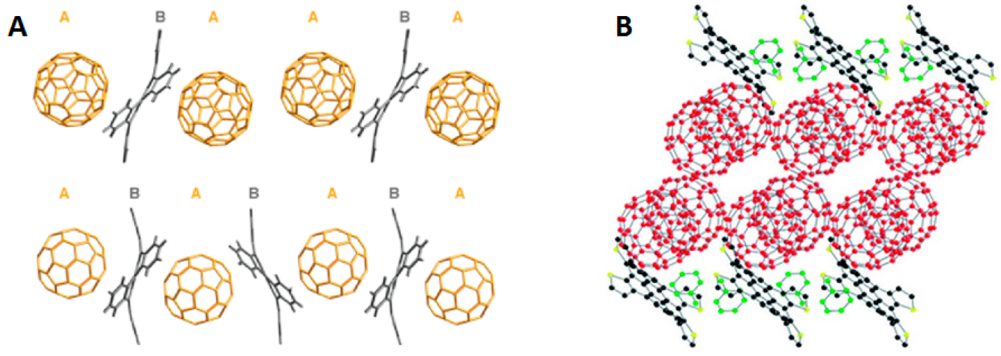

Figure 14. (A) Co-crystals of **1** and C_{60} from solution (top) and from vapor phase (bottom). (B) Co-crystals of a derivative of **2** with C_{60}. Toluene molecules in green. Adapted with permission from ref 10, Copyright 2011 Royal Society of Chemistry, and ref 52, Copyright 2010 WILEY-VCH Verlag GmbH & Co. KGaA.

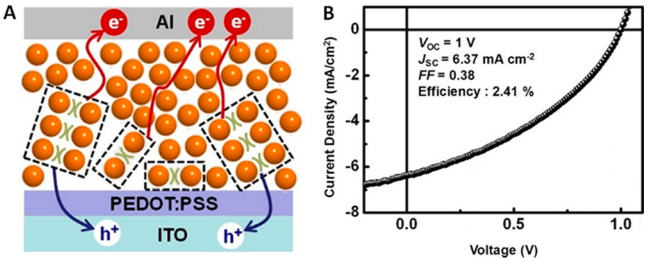

Figure 15. (A) Self-assembled p−n junction of a **1B**:$PC_{70}BM$ film. (B) *J*−*V* characteristics of a 10:90 wt % **1B**/$PC_{70}BM$ device under illumination. Adapted from ref 53. Copyright 2013 American Chemical Society.

the c-HBCs.[11] Further red shifting of the absorbance will likely improve the performance of these materials in OPVs.

These results suggest a new design strategy for solution-processed solar cells to improve device performance by molecular scale self-assembly via noncovalent interaction between a donor and an acceptor. This type of interaction would be difficult to achieve within polymer chemistry. We can increase the strength of the association between fullerenes and these contorted molecules by making them more tightly curved (Figure 13).[44]

N-Type Acceptors from c-PDI

Despite their widespread use, fullerene acceptors have some drawbacks. In general, it is difficult to tune the optical properties and electronic structure of fullerenes over a wide range of energies. As a result, we found that PDI dimer ($\mathbf{4}_2$) functions as an electron acceptor in solar cells.[55] Dimer ($\mathbf{4}_2$) has relatively high electron mobility ($\sim 10^{-2}$ cm^2 V^{-1} s^{-1}), good electron-accepting behavior, and a LUMO energy level similar in magnitude to that of typical fullerenes.[12] The electron donors used are the commercially available polymers polythieno[3,4-*b*]-thiophene-*co*-benzodithiophene (PTB7)[56] and poly[4,8-bis(5-(2-ethylhexyl)thiophen-2-yl)benzo[1,2-

dx.doi.org/10.1021/ar500355d | Acc. Chem. Res. 2015, 48, 267−276

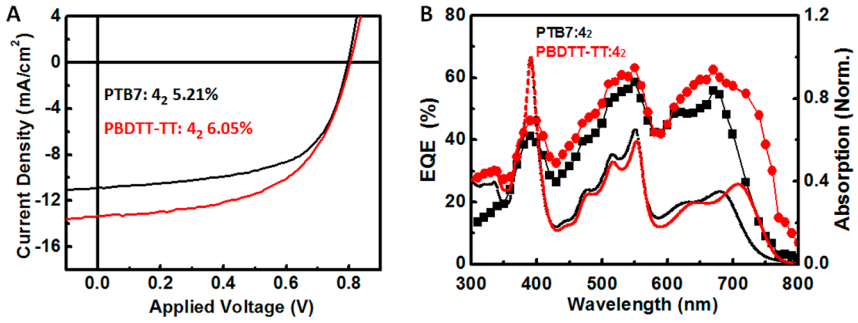

Figure 16. (A) *J*–*V* curves for PTB7:$\mathbf{4}_2$ and PBDTT-TT:$\mathbf{4}_2$ solar cells. (B) EQE spectra (symbols) of PTB7:$\mathbf{4}_2$ (black) and PBDTT-TT:$\mathbf{4}_2$ (red) devices and absorption spectra (lines) for the PTB7:$\mathbf{4}_2$ (black) and PBDTT-TT:$\mathbf{4}_2$ (red) blend films (3:7 D/A mass ratio). Adapted from ref 55. Copyright 2014 American Chemical Society.

b;4,5-b′]dithiophene-2,6-diyl-*alt*-(4-(2-ethylhexyl)-3-fluorothieno[3,4-*b*]thiophene)-2-carboxylate-2,6-diyl] (PBDTT-TT).[57] These donors with $\mathbf{4}_2$ have PCEs of over 6% with simulated solar light, a competitive figure even among some of the best-reported nonfullerene BHJs (Figure 16).[58,59] We observe exciton generation and dissociation at the interface with ultrafast electron transfer from donor to acceptor and hole transfer from acceptor to donor.[55] Ongoing studies are exploring OPVs of the longer oligomers and the relationship between conformation of the ribbons and the device properties. There is a recent publication on using three-dimensional materials in organic devices.[54]

SUMMARY AND OUTLOOK

This Account describes the design, synthesis, and assembly of contorted, polycyclic aromatic compounds. A key finding was that curved pi surfaces of these molecules, like their planar cousins, provide efficacious electronic properties within materials. We found that, in some cases, contorted molecules are efficient at intermolecular charge transport, boding well for their inclusion within materials science.

As described, the disc-shaped molecules have concave surfaces, making them ideal molecular partners with electron-deficient aromatic compounds. We showed that when the disc-shaped molecules are substituted with various hydrocarbons, they self-assemble into either liquid-crystalline films or macroscopic cables. Regardless of assembly, the molecules have noteworthy electronic properties and form hole-transporting materials in OFET devices. Shape complementarity between the concave, electron-rich, disc-shaped materials coupled with electron-deficient spherical molecules was explored. The ball and socket motif resulted in approximately a two orders of magnitude increase in efficiency in photovoltaics devices relative to that of devices that lack this motif.

We also sought to provide insight on the synthesis and electronic properties of ribbon-shaped molecules that can be conceptualized as ribbons of graphene. In solar cells, these contorted ribbons with commercial donor polymers have record efficiencies for non-fullerene-based solar cells. Given the knowledge acquired studying the contorted, disc-shaped molecules, an area of future research surrounds how to couple these efficacious n-type materials with electron-donating partners, forming a well-defined interface similar to the ball-and-socket motif.

AUTHOR INFORMATION

Corresponding Authors

*(F.N.) E-mail: fwn2@columbia.edu.
*(M.S.) E-mail: mls2064@columbia.edu.
*(S.X.) E-mail: senksong@msn.com.
*(C.N.) E-mail: cn37@columbia.edu.

Notes

The authors declare no competing financial interest.

Biographies

Melissa Ball was born in Chattanooga, Tennessee, in 1981. She holds an undergraduate degree in economics from Hunter College, City University of New York, and a Masters degree in Political Economy from the London School of Economics. She is currently a first year graduate student in Chemistry at Columbia University with Colin Nuckolls.

Yu Zhong was born in Hubei, China, in 1988. He did his undergraduate training at the University of Science and Technology of China (USTC) with Beifang Yang and Shuhong Yu. He is a Ph.D. student in the Department of Chemistry at Columbia University with Colin Nuckolls. His research interests include organic field effect transistors and photovoltaics.

Ying Wu was born in Zhejiang, China, in 1988. She did her undergraduate training at the University of Science and Technology of China (USTC) with Guangzhao Zhang. She is now a fifth year graduate student in the Nuckolls lab, studying the synthesis and application of supersized contorted aromatics.

Christine Schenck was born in Orange County, New York, in 1986. She received her undergraduate training from Marist College in Poughkeepsie, New York, studying with Jocelyn Nadeau. Christine received her Ph.D. in 2013 from Columbia University with Colin Nuckolls. She has since joined the Upper Division faculty at Horace Mann School in Bronx, New York.

Fay Ng was born in Guangzhou, China, in 1969. She did her undergraduate training at UCLA and her graduate training at Columbia with Samuel Danishefsky. She was an NIH postdoctoral fellow with Larry Overman at UC Irvine. She has been at Columbia since 2005 as a research scientist and instructor.

Michael Steigerwald was born in Michigan in 1956. He did both his undergraduate and graduate training at Caltech, working with Dave Evans, Bill Goddard, and Bob Grubbs. After a postdoc with Marty Semmelhack at Princeton, he joined Bell Laboratories, where he worked in solid-state chemistry. He has been at Columbia since 2002 as a research scientist.

Shengxiong Xiao was born in Hubei, China, in 1977. He completed his undergraduate studies at Wuhan University, China, in 1999. He received his M.S. degree from the Institute of Chemistry, Chinese Academy of Sciences, under the guidance of Profs. Yuliang Li and Daoben Zhu in 2002. He received his Ph.D. in 2007 with Prof. Colin Nuckolls and then was a postdoctoral fellow with Julius Rebek, Jr. at the Scripps Research Institute. He joined the faculty at Shanghai Normal University, China, in 2012 and was appointed as an Eastern Scholar Professor of Shanghai City in 2013.

Colin Nuckolls was born at Lakenheath RAF in Great Britain in 1970. He completed his undergraduate studies at the University of Texas at Austin, studying with Marye Anne Fox, and then received his Ph.D. in 1998 from Columbia University with Thomas Katz. He was an NIH postdoctoral fellow with Julius Rebek, Jr. at the Scripps Research Institute. He joined the faculty at Columbia University in 2000, and in 2006, he was promoted to the rank of Professor.

■ ACKNOWLEDGMENTS

We thank all co-workers and collaborators that studied contorted aromatics. M.B. thanks Mitchell Ball for teaching her the value of hard work. We thank the long-term support for this project provided by the Chemical Sciences, Geosciences and Biosciences Division, Office of Basic Energy Sciences, US Department of Energy (DOE) under award number DE-FG02-01ER15264. S.X. thanks NSFC (21473113), Shanghai Municipal Science and Technology Commission (no. 12 nm0504000), Program for Professor of Special Appointment (Eastern Scholar) at Shanghai Institutions of Higher Learning (no. 2013-57), Program for Changjiang Scholars and Innovative Research Team in University (IRT1269), and International Joint Laboratory on Resource Chemistry (IJLRC) for financial support.

■ REFERENCES

(1) Akasaka, T.; Wudl, F.; Nagase, S. *Chemistry of Nanocarbons*; Wiley: Chichester, West Sussex, 2010.
(2) Wu, J.; Pisula, W.; Müllen, K. Graphenes as potential material for electronics. *Chem. Rev.* **2007**, *107*, 718−747.
(3) Omachi, H.; Segawa, Y.; Itami, K. Synthesis of cycloparaphenylenes and related carbon nanorings: a step toward the controlled synthesis of carbon nanotubes. *Acc. Chem. Res.* **2012**, *45*, 1378−1389.
(4) Jasti, R.; Bhattacharjee, J.; Neaton, J. B.; Bertozzi, C. R. Sythesis, characterization, and theory of [9]-,[12]-, and [18]-cycloparaphenylene: carbon nanohoop structures. *J. Am. Chem. Soc.* **2008**, *130*, 17646−17647.
(5) Petrukhina, M. A.; Scott, L. T.; Kroto, H. W. *Fragments of Fullerenes and Carbon Nanotubes: Designed Synthesis, Unusual Reactions, and Coordination Chemistry*; Wiley: Chichester, West Sussex, 2011.
(6) Bendikov, M.; Wudl, F.; Perepichka, D. F. Tetrathiafulvalenes, oligoacenenes, and their buckminsterfullerene derivatives: the brick and mortar of organic electronics. *Chem. Rev.* **2004**, *104*, 4891−4945.
(7) Gingras, M. One hundred years of helicene chemistry. Part 1: non-stereoselective syntheses of carbohelicenes. *Chem. Soc. Rev.* **2013**, *42*, 968−1006.
(8) Grimme, S.; Peyerimhoff, S. D. Theoretical study of the structures and racemization barriers of [*n*]helicenes (*n* = 3−6, 8). *Chem. Phys.* **1996**, *204*, 411−417.
(9) Xiao, S.; Myers, M.; Miao, Q.; Sanaur, S.; Pang, K.; Steigerwald, M. L.; Nuckolls, C. Molecular wires from contorted aromatic compounds. *Angew. Chem., Int. Ed.* **2005**, *44*, 7390−7394.
(10) Chiu, C. Y.; Kim, B.; Gorodetsky, A. A.; Sattler, W.; Wei, S.; Sattler, A.; Steigerwald, M.; Nuckolls, C. Shape-shifting in contorted dibenzotetrathienocoronenes. *Chem. Sci.* **2011**, *2*, 1480−1486.
(11) Xiao, S.; Kang, S. J.; Wu, Y.; Ahn, S.; Kim, J. B.; Loo, Y. L.; Siegrist, T.; Steigerwald, M. L.; Li, H. X.; Nuckolls, C. Supersized contorted aromatics. *Chem. Sci.* **2013**, *4*, 2018−2023.
(12) Zhong, Y.; Kumar, B.; Oh, S.; Trinh, M. T.; Wu, Y.; Elbert, K.; Li, P.; Zhu, X.; Xiao, S.; Ng, F.; Steigerwald, M. L.; Nuckolls, C. Helical ribbons for molecular electronics. *J. Am. Chem. Soc.* **2014**, *136*, 8122−8130.
(13) Clar, E.; Stephen, J. F. The synthesis of 1:2, 3:4, 5:6, 7:8, 9:10, 11:12-hexabenzocoronene. *Tetrahedron* **1965**, *21*, 467−470.
(14) Zhang, Q.; Peng, H.; Zhang, G.; Lu, Q.; Chang, J.; Dong, Y.; Shi, X.; Wei, J. Facile bottom-up synthesis of coronene-based 3-fold symmetrical and highly substituted nanographenes from simple aromatics. *J. Am. Chem. Soc.* **2014**, *136*, 5057−5064.
(15) Chen, L.; Mali, K. S.; Puniredd, S. R.; Baumgarten, M.; Parvez, K.; Pisula, W.; De Feyter, S.; Müllen, K. Assembly and fiber formation of a gemini-type hexathienocoronene amphiphile for electrical conduction. *J. Am. Chem. Soc.* **2013**, *135*, 13531−13537.
(16) Chen, L.; Puniredd, S. R.; Tan, Y.-Z.; Baumgarten, M.; Zschieschang, U.; Enkelmann, V.; Pisula, W.; Feng, X.; Klauk, H.; Müllen, K. Hexathienocoronenes: synthesis and self-organization. *J. Am. Chem. Soc.* **2012**, *134*, 17869−17872.
(17) Arslan, H.; Uribe-Romo, F. J.; Smith, B. J.; Dichtel, W. R. Accessing extended and partially fused hexabenzocoronenes using a benzannulation/cyclodehydrogenation approach. *Chem. Sci.* **2013**, *4*, 3973−3978.
(18) He, B.; Pun, A. B.; Klivansky, L. M.; McGough, A. M.; Ye, Y.; Zhu, J.; Guo, J.; Teat, S. J.; Liu, Y. Thiophene fused azacoronenes: regioselective synthesis, self-organization, charge transport and its incorporation in conjugated polymers. *Chem. Mater.* **2014**, *26*, 3920−3927.
(19) Cohen, Y. S.; Xiao, S.; Steigerwald, M. L.; Nuckolls, C.; Kagan, C. R. Enforced one-dimensional photoconductivity in core-cladding hexabenzocoronenes. *Nano Lett.* **2006**, *6*, 2838−2841.
(20) Hauptmann, S.; Clar, V. E. Aromaticity—change in meaning of a term. *Z. Chem.* **1973**, *13*, 361−364.
(21) Loo, Y. L.; Hiszpanski, A. M.; Kim, B.; Wei, S. J.; Chiu, C. Y.; Steigerwald, M. L.; Nuckolls, C. Unusual molecular conformations in fluorinated, contorted hexabenzocoronenes. *Org. Lett.* **2010**, *12*, 4840−4843.
(22) Kang, S. J.; Kim, J. B.; Chiu, C. Y.; Ahn, S.; Schiros, T.; Lee, S. S.; Yager, K. G.; Toney, M. F.; Loo, Y. L.; Nuckolls, C. A supramolecular complex in small-molecule solar cells based on contorted aromatic molecules. *Angew. Chem., Int. Ed.* **2012**, *51*, 8594−8597.
(23) Roncali, J. Conjugated poly(thiophenes)—synthesis, functionalization, and applications. *Chem. Rev.* **1992**, *92*, 711−738.
(24) Anthony, J. E. Functionalized acenes and heteroacenes for organic electronics. *Chem. Rev.* **2006**, *106*, 5028−5048.
(25) Chebny, V. J.; Gwengo, C.; Gardinier, J. R.; Rathore, R. Synthesis and electronic properties of iso-alkyl substituted hexa-peri-hexabenzocoronenes (HBC's) from a versatile new HBC synthon, hexakis(4-acetylphenyl)benzene. *Tetrahedron Lett.* **2008**, *49*, 4869−4872.
(26) Schiros, T.; Mannsfeld, S.; Chiu, C. Y.; Yager, K. G.; Ciston, J.; Gorodetsky, A. A.; Palma, M.; Bullard, Z.; Kramer, T.; Delongchamp, D.; Fischer, D.; Kymissis, I.; Toney, M. F.; Nuckolls, C. Reticulated organic photovoltaics. *Adv. Funct. Mater.* **2012**, *22*, 1167−1173.
(27) Gorodetsky, A. A.; Chiu, C. Y.; Schiros, T.; Palma, M.; Cox, M.; Jia, Z.; Sattler, W.; Kymissis, I.; Steigerwald, M.; Nuckolls, C. Reticulated heterojunctions for photovoltaic devices. *Angew. Chem., Int. Ed.* **2010**, *49*, 7909−7912.
(28) Jiang, W.; Li, Y.; Wang, Z. Tailor-made rylene arrays for high performance n-channel semiconductors. *Acc. Chem. Res.* **2014**, *47*, 3135−3147.
(29) Kastler, M.; Pisula, W.; Laquai, F.; Kumar, A.; Davies, R. J.; Baluschev, S.; Garcia−Gutiérrez, M. C.; Wasserfallen, D.; Butt, H. J.; Riekel, C.; Wegner, G.; Müllen, K. Organization of charge-carrier pathways for organic electronics. *Adv. Mater.* **2006**, *18*, 2255−2259.

(30) Schmaltz, B.; Weil, T.; Müllen, K. Polyphenylene-based materials: control of the electronic function by molecular and supramolecular complexity. *Adv. Mater.* **2009**, *21*, 1067−1078.
(31) Xiao, S.; Tang, J.; Beetz, T.; Guo, X.; Tremblay, N.; Siegrist, T.; Zhu, Y.; Steigerwald, M.; Nuckolls, C. Transferring self-assembled, nanoscale cables into electrical devices. *J. Am. Chem. Soc.* **2006**, *128*, 10700−10701.
(32) Xiao, S.; Kang, S. J.; Zhong, Y.; Zhang, S.; Scott, A. M.; Moscatelli, A.; Turro, N. J.; Steigerwald, M. L.; Li, H.; Nuckolls, C. Controlled doping in thin-film transistors of large contorted aromatic compounds. *Angew. Chem., Int. Ed.* **2013**, *52*, 4558−4562.
(33) Wurthner, F.; Stolte, M. Naphthalene and perylene diimides for organic transistors. *Chem. Commun.* **2011**, *47*, 5109−5115.
(34) Zhao, Y.; Guo, Y. L.; Liu, Y. 25th Anniversary Article: Recent advances in n-type and ambipolar organic field-effect transistors. *Adv. Mater.* **2013**, *25*, 5372−5391.
(35) Guo, X.; Small, J. P.; Klare, J. E.; Wang, Y.; Purewal, M. S.; Tam, I. W.; Hong, B. H.; Caldwell, R.; Huang, L.; O'Brien, S.; Yan, J.; Breslow, R.; Wind, S. J.; Hone, J.; Kim, P.; Nuckolls, C. Covalently bridging gaps in single-walled carbon nanotubes with conducting molecules. *Science* **2006**, *311*, 356−359.
(36) Feldman, A. K.; Steigerwald, M. L.; Guo, X.; Nuckolls, C. Molecular electronic devices based on single-walled carbon nanotube electrodes. *Acc. Chem. Res.* **2008**, *41*, 1731−1741.
(37) Guo, X.; Xiao, S.; Myers, M.; Miao, Q.; Steigerwald, M. L.; Nuckolls, C. Photoresponsive nanoscale columnar transistors. *Proc. Natl. Acad. Sci. U.S.A.* **2009**, *106*, 691−696.
(38) Guo, X.; Myers, M.; Xiao, S.; Lefenfeld, M.; Steiner, R.; Tulevski, G. S.; Tang, J.; Baumert, J.; Leibfarth, F.; Yardley, J. T.; Steigerwald, M. L.; Kim, P.; Nuckolls, C. Chemoresponsive monolayer transistors. *Proc. Natl. Acad. Sci. U.S.A.* **2006**, *103*, 11452−11456.
(39) Eom, D.; Prezzi, D.; Rim, K. T.; Zhou, H.; Lefenfeld, M.; Xiao, S.; Nuckolls, C.; Hybertsen, M. S.; Heinz, T. F.; Flynn, G. W. Structure and electronic properties of graphene nanoislands on Co(0001). *Nano Lett.* **2009**, *9*, 2844−2848.
(40) Prezzi, D.; Eom, D.; Rim, K. T.; Zhou, H.; Xiao, S.; Nuckolls, C.; Heinz, T. F.; Flynn, G. W.; Hybertsen, M. S. Edge structures for nanoscale graphene islands on Co(0001) surfaces. *ACS Nano* **2014**, *8*, 5765−5773.
(41) Treier, M.; Ruffieux, P.; Groning, P.; Xiao, S.; Nuckolls, C.; Fasel, R. An aromatic coupling motif for two-dimensional supramolecular architectures. *Chem. Commun.* **2008**, 4555−4557.
(42) Rim, K. T.; Siaj, M.; Xiao, S.; Myers, M.; Carpentier, V. D.; Liu, L.; Su, C.; Steigerwald, M. L.; Hybertsen, M. S.; McBreen, P. H.; Flynn, G. W.; Nuckolls, C. Forming aromatic hemispheres on transition-metal surfaces. *Angew. Chem., Int. Ed.* **2007**, *46*, 7891−7895.
(43) Sanchez-Valencia, J. R.; Dienel, T.; Groning, O.; Shorubalko, I.; Mueller, A.; Jansen, M.; Amsharov, K.; Ruffieux, P.; Fasel, R. Controlled synthesis of single-chirality carbon nanotubes. *Nature* **2014**, *512*, 61−64.
(44) Whalley, A. C.; Plunkett, K. N.; Gorodetsky, A. A.; Schenck, C. L.; Chiu, C. Y.; Steigerwald, M. L.; Nuckolls, C. Bending contorted hexabenzocoronene into a bowl. *Chem. Sci.* **2011**, *2*, 132−135.
(45) Miller, N. C.; Sweetnam, S.; Hoke, E. T.; Gysel, R.; Miller, C. E.; Bartelt, J. A.; Xie, X.; Toney, M. F.; McGehee, M. D. Molecular packing and solar cell performance in blends of polymers with a bisadduct fullerene. *Nano Lett.* **2012**, *12*, 1566−1570.
(46) Mayer, A. C.; Toney, M. F.; Scully, S. R.; Rivnay, J.; Brabec, C. J.; Scharber, M.; Koppe, M.; Heeney, M.; McCulloch, I.; McGehee, M. D. Bimolecular crystals of fullerenes in conjugated polymers and the implications of molecular mixing for solar cells. *Adv. Funct. Mater.* **2009**, *19*, 1173−1179.
(47) Cates, N. C.; Gysel, R.; Beiley, Z.; Miller, C. E.; Toney, M. F.; Heeney, M.; McCulloch, I.; McGehee, M. D. Tuning the properties of polymer bulk heterojunction solar cells by adjusting fullerene size to control intercalation. *Nano Lett.* **2009**, *9*, 4153−4157.
(48) Kennedy, R. D.; Ayzner, A. L.; Wanger, D. D.; Day, C. T.; Halim, M.; Khan, S. I.; Tolbert, S. H.; Schwartz, B. J.; Rubin, Y. Self-assembling fullerenes for improved bulk-heterojunction photovoltaic devices. *J. Am. Chem. Soc.* **2008**, *130*, 17290−17292.
(49) Bürckstümmer, H.; Tulyakova, E. V.; Deppisch, M.; Lenze, M. R.; Kronenberg, N. M.; Gsänger, M.; Stolte, M.; Meerholz, K.; Würthner, F. Efficient solution-processed bulk heterojunction solar cells by antiparallel supramolecular arrangement of dipolar donor-acceptor dyes. *Angew. Chem., Int. Ed.* **2011**, *50*, 11628−11632.
(50) Troshin, P. A.; Sariciftci, N. S. Supramolecular chemistry for organic photovoltaics. In *Supramolecular Chemistry: From Molecules to Nanomaterials*; Gale, P. A.; Steed, J. W., Eds.; John Wiley & Sons: Hoboken, NJ, 2012.
(51) Loser, S.; Bruns, C. J.; Miyauchi, H.; Ortiz, R. P.; Facchetti, A.; Stupp, S. I.; Marks, T. J. A naphthodithiophene-diketopyrrolopyrrole donor molecule for efficient solution-processed solar cells. *J. Am. Chem. Soc.* **2011**, *133*, 8142−8145.
(52) Tremblay, N. J.; Gorodetsky, A. A.; Cox, M. P.; Schiros, T.; Kim, B.; Steiner, R.; Bullard, Z.; Sattler, A.; So, W. Y.; Itoh, Y.; Toney, M. F.; Ogasawara, H.; Ramirez, A. P.; Kymissis, I.; Steigerwald, M. L.; Nuckolls, C. Photovoltaic universal joints: ball-and-socket interfaces in molecular photovoltaic cells. *ChemPhysChem* **2010**, *11*, 799−803.
(53) Kang, S. J.; Ahn, S.; Kim, J. B.; Schenck, C.; Hiszpanski, A. M.; Oh, S.; Schiros, T.; Loo, Y. L.; Nuckolls, C. Using self-organization to control morphology in molecular photovoltaics. *J. Am. Chem. Soc.* **2013**, *135*, 2207−2212.
(54) Skabara, P. J.; Arlin, J.-B.; Geerts, Y. H. Close encounters of the 3D kind—exploiting high dimensionality in molecular semiconductors. *Adv. Mater.* **2013**, *25*, 1948−1954.
(55) Zhong, Y.; Trinh, M. T.; Chen, R.; Wang, W.; Khlyabich, P. P.; Kumar, B.; Xu, Q.; Nam, C. Y.; Sfeir, M. Y.; Black, C.; Steigerwald, M. L.; Loo, Y. L.; Xiao, S.; Ng, F.; Zhu, X.; Nuckolls, C. Efficient organic solar cells with helical perylene diimide electron acceptors. *J. Am. Chem. Soc.* **2014**, *136*, 15215−15221.
(56) Liang, Y.; Xu, Z.; Xia, J.; Tsai, S.-T.; Wu, Y.; Li, G.; Ray, C.; Yu, L. For the bright future-bulk heterojunction polymer solar cells with power conversion efficiency of 7.4%. *Adv. Mater.* **2010**, *22*, E135−E138.
(57) Liao, S.-H.; Jhuo, H.-J.; Cheng, Y.-S.; Chen, S.-A. Fullerene derivative-doped zinc oxide nanofilm as the cathode of inverted polymer solar cells with low-bandgap polymer (PTB7-Th) for high performance. *Adv. Mater.* **2013**, *25*, 4766−4771.
(58) Zang, Y.; Li, C.-Z.; Chueh, C.-C.; Williams, S. T.; Jiang, W.; Wang, Z.-H.; Yu, J.-S.; Jen, A. K. Y. Integrated molecular, interfacial, and device engineering towards high-performance non-fullerene based organic solar cells. *Adv. Mater.* **2014**, *26*, 5708−5714.
(59) Lu, Z.; Jiang, B.; Zhang, X.; Tang, A.; Chen, L.; Zhan, C.; Yao, J. Perylene-diimide based non-fullerene solar cells with 4.34% efficiency through engineering surface donor/acceptor compositions. *Chem. Mater.* **2014**, *26*, 2907−2914.